

24th COBEM - 2017



24th ABCM International Congress of Mechanical Engineering
December 3-8, 2017, Curitiba, PR, Brazil

COBEM-2017-0403

DISTRIBUTED MODEL TO ACHIEVE THE STEADY STATE THROUGH THE FALSE TRANSIENT IN A SOLAR ASSISTED HEAT PUMP

Tiago de Freitas Paulino

Graduate Program in Mechanical Engineering, Federal University of Minas Gerais, Av. Antônio Carlos , 6627, Pampulha, 31270-901, Belo Horizonte (MG), Brazil

Department of Materials Engineering, Federal Center of Technological Education of Minas Gerais, Av. Amazonas, 5253, Nova Suíça, 30421-169, Belo Horizonte (MG), Brazil
tfpaulinoeng@gmail.com

Raphael Nunes de Oliveira

Department of Mechanical Engineering, Federal Center of Technological Education of Minas Gerais, Av. Amazonas, 7675, Nova Gameleira, 30510-000, Belo Horizonte (MG), Brazil
rphnunes@gmail.com

Luiz Machado

Ricardo Nicolau Nassar Koury

Graduate Program in Mechanical Engineering, Federal University of Minas Gerais, Av. Antônio Carlos , 6627, Pampulha, 31270-901, Belo Horizonte (MG), Brazil
luizm@demec.ufmg.br, koury@demec.ufmg.br

Abstract. *In this study, the distributed model of a direct expansion solar assisted CO₂ heat pump are used. The methodology shows that it is possible for the system to achieve the correct steady state without it passing through a real transient, with the false transient operating during the initial part of the process. It is shown that, regardless of the initial temperature and mass distribution in the evaporator, if all points are in the same isochoric, then the same steady state will be achieved through the false transient. The isochoric of 0.00384 m³/kg was chosen and two points on this curve are used. The total mass are 120 grams in both points. The results show that the same evaporating temperature around 14.5°C and the superheat of 6 °C, was achieved in the steady state. Moreover, the liquid mass is 52 grams and the vapor mass is 68 grams in the steady state. The results of the simulation of the false transient were compared with the results achieve through the real transient simulation demonstrate a good agreement. Therefore, this methodology is appropriate to achieve the steady state in a simpler manner.*

Keywords: *mathematical model, false transient, steady state, CO₂ heat pump, solar assisted*

1. INTRODUCTION

The detailed knowledge about the characteristics of the operation in the transient and steady state, in a heat pump, can be achieved by experimental simulation and by the mathematical model. Having a mathematical model able to represent accurately the system, a lower time is required to achieve a great number of operation points in comparison with experimental simulations.

Excluding the black box models that are created by the experimental simulations, the options for mathematical models of evaporators can be divided into the lamped model (Navarro-Esbri *et al.*, 2010; Salazar and Mendes, 2014), the moving boundary model (Zhou *et al.*, 2010; Esbri *et al.*, 2015) and the distributed model (Moreno-Rodríguez *et al.*, 2012; Faria *et al.*, 2016). These models can be obtained by the equations of continuity, energy and momentum. In the lamped model, only one value of each property of the refrigerant in the evaporator is used. In the moving boundary model the refrigerant properties and correlations is analyzed in separate for the boiling and the superheat region. Finally, in the distributed model the evaporator is divided into various small control volumes. Since the equations of continuity, energy, momentum and heat transfer are defined in each control volume, compared to the lamped model and the moving boundary model, the physics problem is better represented in the distributed model.

In general, a direct expansion solar assisted heat pump (DX-SAHP) works in the transient operations during initial part of the process and during ambient conditions variations on the system, e.g. the variations of solar radiation, ambient

temperature and wind velocity. In some case, it could be important the knowledge of equipment behaviour when the operation is in the steady state and some aspect of the environment change. Therefore, for this situation the start-up of the equipment is not important, but the knowledge about the steady state is essential. Reaching the steady state one ambient conditions could be changed and a new steady state will be reached.

In the present study, a distributed model of a DX-SAHP evaporator is used to analyse an alternative to achieve the steady state during the start-up of the system. The proposal of this study is that the correct steady state will be reached without the system passing through a real transient, instead of this, the false transient operating during the start-up of the process. This approach could be used in situations where the knowledge about transient is of little interest.

2. MATHEMATICAL MODEL

Figure 1 shows the main components at this DX-SAHP: a needle valve as an expansion device (1), an evaporator/collector (2), a reciprocating compressor (3) and a gas cooler (4). The refrigerant is Carbon dioxide (CO₂). This heat pump was developed to produce sanitary hot water for a family with four people. The hot water is storage in a thermal energy storage and the variables have been considered constant at the gas cooler. Faria *et al.* (2016) experimentally validates the distributed model used in this study for the DX-SAHP.

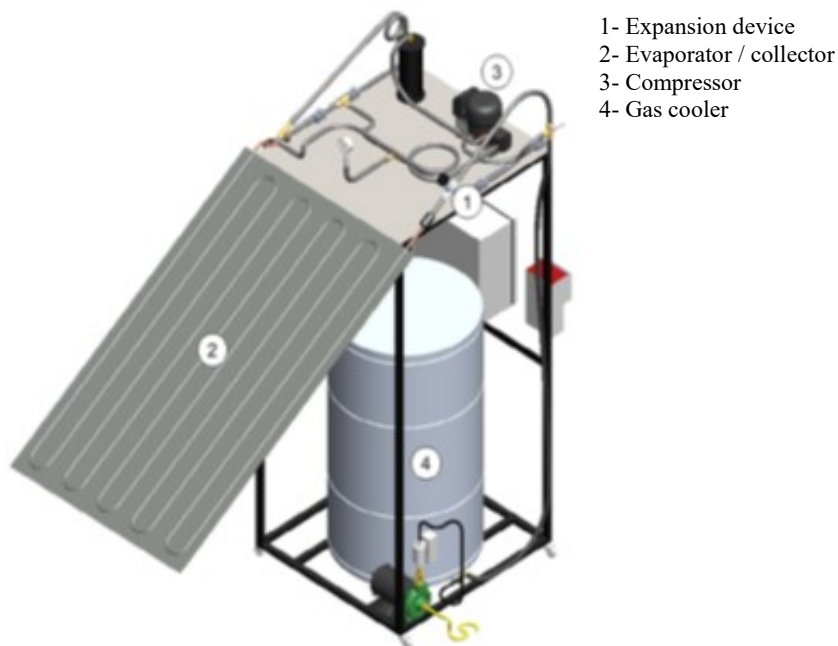


Figure 1. CO₂ DX-SAHP for water heating.

2.1 Evaporator / collector

The evaporator / collector receives energy from natural and forced convection, from the condensation of water vapor in the external atmospheric air and from solar radiation. Tab. 1 shows the main characteristics and parameters of the evaporator / collector.

Table 1. Characteristics and parameters of the evaporator/ collector.

Geometry	Absorber(fins) and coil (tube)
Tube and fins	Cooper
Secondary fluid	Air
Tube diameters (out/in)	$D_o = 7.6$ mm and $D_i = 6.0$ mm
Coil length	$L = 16.3$ m
Distance between tubes	$W = 0.10$ m
Fin thickness	$\delta_{fin} = 1.0$ mm
Fin efficiency	$\eta_{fin} = 0.98$
Plate area	$A = 1.57$ m ²

In order to model the evaporator it is necessary to consider some simplifying assumptions. These assumptions include considering: (i) in the boiling region the liquid and vapor are in thermodynamic equilibrium; (ii) unidirectional refrigerant flow; (iii) no axial heat conduction; (iv) physical properties of the CO₂ and copper are uniform in each tube cross section; (v) negligible resistance of contact between the coil and absorber; (iv) and finally, negligible resistance of the wall tube. Based upon these assumptions the balances of energy, mass and moment for the refrigerant is presented in Eq. (1), (2) and (3), while the balance of energy for the coil is presented in Eq. (4):

$$A_f \frac{\partial}{\partial t} [\rho_f (h_f - P_f v_f)] = -A_f \frac{\partial}{\partial z} (G_f h_f) + H_f p_f (T_w - T_f) \quad (1)$$

$$\frac{\partial \rho_f}{\partial t} + \frac{\partial G_f}{\partial z} = 0 \quad (2)$$

$$\frac{\partial}{\partial t} \left\{ P_f + G_f^2 \left[\frac{x^2 v_v}{\alpha} + \frac{(1-x)^2 v_l}{1-\alpha} \right] \right\} = -\frac{\partial G_f}{\partial t} - \left(\frac{dP}{dz} \right)_{fr} - g \rho_f \sin(\theta) \quad (3)$$

$$\rho_w A_w c_{pw} \frac{\partial T_w}{\partial t} = [(W - D_0) F + D_0] [S - U_L (T_w - T_{sky})] - H_f A_f (T_w - T_f) \quad (4)$$

Where:

A	plate area [m ²]
c _p	specific heat at constant pressure [J.kg ⁻¹ .K ⁻¹]
D ₀	external diameter [m]
f	refrigerant
F	fin efficiency
g	acceleration of gravity [m.s ⁻²]
G	mass velocity [kg.s ⁻¹ .m ⁻²]
H _f	heat transfer coefficient between the wall and the refrigerant [W.m ⁻² .K ⁻¹]
p	perimeter [m]
S	solar radiation [W.m ⁻²]
T	temperature [K]
sky	sky
T	temperature [K]
U _L	combined coefficient involving radiation and convection between the absorber / coil and the environment [W.m ⁻² .K ⁻¹]
v _f	liquid specific volume [m ³ .kg ⁻¹]
v _v	vapor specific volume [m ³ .kg ⁻¹]
x	quality
w	tube wall
W	distance between the centers of two adjacent tubes [m]
(dP/dZ) _{fr}	refrigerant pressure loss by friction [Pa]
α	void fraction
θ	inclination of the absorber relative to the horizontal

The correlations used in equations to calculate heat transfer, void fraction and pressure loss are: (i) H_f in the boiling region as proposed by Cheng et al. (2006) and Cheng et al. (2008); and in superheating region with equation of Dittus-Boelter, presented by Incropera and DeWitt (2002); (ii) void fraction as proposed by Rouhani and Axelsson (1970); (iii) pressure loss in the boiling region as proposed by Fridel and recommended by Cheng et al (2008) and in superheating region with equation of Fanning, described by Ozisik (1985); (iv) U_L in the natural convection part is obtained as proposed by Palyvos (2008), and the condensation part is determined as presented by Huhtiniemi and Corradini (1993); and (v) the equations used to obtain the direct and diffuse radiation and the heat exchange by infrared radiation are calculated as proposed by Duffie and Beckman (2006) and Kalogirou (2009). For more details, see Faria et al. (2016).

2.2 Discretization of the evaporator / collector equations

The time-dependent and spatial-dependent derivatives in the refrigerant equations were determined from the Eq. (5) and (6) respectively:

$$\frac{\partial y}{\partial t} = \frac{y - y^0}{\Delta t} \quad (5)$$

$$\frac{\partial y}{\partial z} = \frac{y_o - y_i}{\Delta z} \quad (6)$$

The subscripts i and o represent the control volume inlet and outlet respectively. The dependent variable y can be temperature, pressure, enthalpy, density, mass flow rate, etc. The variables t and z are the time and the spatial position respectively. And the superscripts 0 represents the values of the variables at the instant of time $t-\Delta t$.

2.3 Simulation methodology

In order to demonstrate that this is a useful methodology, it is shown that, regardless of the initial temperature and mass distribution in the evaporator, if all points are in the same isochoric, then the same steady state will be achieved through the false transient. For this purpose, the following simulation conditions were established: the inlet and the outlet mass flow rate in the evaporator are equal, the enthalpy in the entrance of the evaporator and the environment conditions are constant, these are the model boundary conditions. After that, the initial conditions are given: temperature and enthalpy along the evaporator. Then, two convergences criterions of the model are assumed: the spatial profile of the evaporator wall temperature and the inlet pressure of the evaporator. Therefore, the enthalpy, the mass velocity and pressure, all of them at the evaporator inlet have been used as input in the first control volume and through the Eq. (1), (2) and (3) the output data are calculated. Then, this data are the input for the next control volume and this procedure is used in all evaporator. The evaporator model was run with 2000 control volumes and a time step of 2 seconds. However, the correlations used in the boiling and superheat regions are different as discussed in the evaporator model. Thus, if the mass velocity imposed by the boundary conditions is not equal to the mass velocity calculated by Eq. (2), the inlet evaporator pressure need to be changed. After the second interaction, the Newton-Raphson algorithm is used to accelerate the convergence between the mass velocities (within a defined error margin). The second step of the model is the calculation of the spatial profile of the tube wall temperature by Eq. (4). The procedure for calculating refrigerant properties is repeated until the convergence of the tube wall temperature. Figure 2 shows the model flow chart above described. The software used is the Fortran program. The CO₂ properties were estimated using the equations proposed by Span and Wagner (1996).

2.4 Data of simulation

The isochoric of 0.00384 m³/kg was chosen and two points on this curve are used as shows Tab. 2. First column presents the points. The second, third and fourth columns contain the number of control volumes with only liquid, the number of control volumes with only vapor and the sum of control volumes respectively. Fifth column reports the initial evaporating temperature. The sixth, seventh and eighth columns contains the mass of liquid, the mass of vapor and the total mass respectively. These data are used with entrance data in the model. It is important to highlight with Points 1 and 2 have the same specific volume and total mass. Therefore the mass flow rate is 30 kg/h, as well as being considered equal in the expansion device and compressor as discussed, the mass flow rate is also consider constant during all the false transient simulations.

Table 2. Initial conditions.

Point	Number control volumes			Temperature (°C)	Mass (g)		
	Liq.	Vap.	Total		Liq.	Vap.	Total
1	206	1794	2000	21.2	36	84	120
2	284	1716	2000	16.6	52.8	67.2	120

3. RESULTS AND DISCUSSION

Figure 3 shows the results for Point 1 in the Tab. 2. The initial evaporating temperature is 21.2 °C and the initial superheat is 0°C.

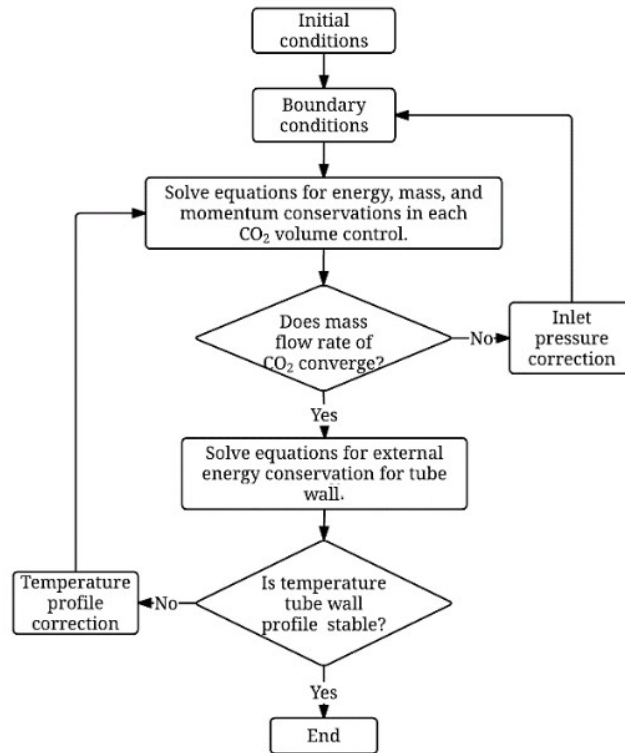


Figure 2. Model flow chart.

Then, the steady state have the evaporating temperature and the superheat around 14.5 °C and 6 °C respectively. In the same way, Figure 4 shows the results for Point 2. The initial evaporating temperature is 16.6 °C and the initial superheat is 0 °C. Therefore in the steady state the evaporating temperature is around 14.5 °C and the superheat is around 6 °C. In brief, in the steady state, the same evaporating temperature and superheat are achieved for Points 1 and 2 in the false transient simulation.

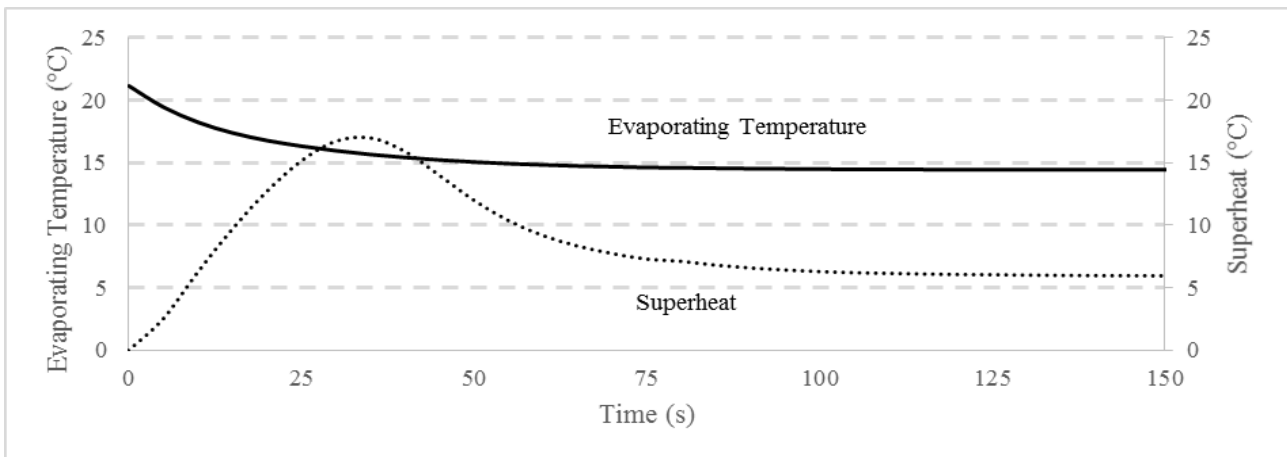


Figure 3. False Transient - Evaporating Temperature and Superheat – Point 1.

In addition it is important compare the results achieved by the false transient simulation and the real transient simulation. Then, the real transient simulation is performed and the same values are found in the steady state for superheat and evaporating temperature. As a result, if the system has the same environment conditions, the inlet and outlet evaporator mass flow rate is the same and the same mass is consider in the evaporator, a single steady state will be reached, regardless of the initial values chosen for the refrigerant temperature and liquid-vapor spatial distribution. Furthermore, it is important to highlight that in the Figures 3 and 4 the evolution over time during the false transient is not real, however the values in the steady state are.

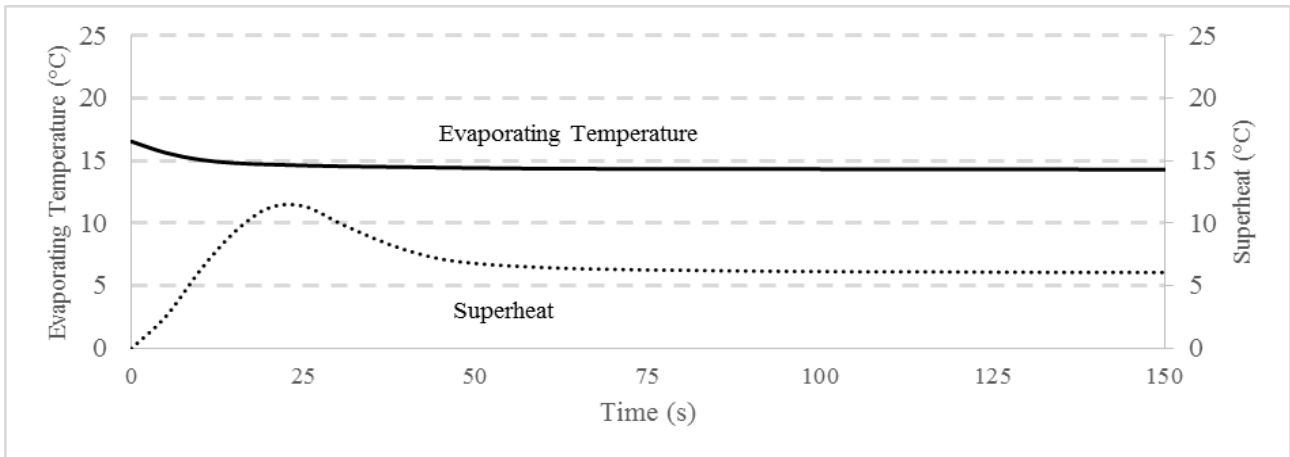


Figure 4. False Transient - Evaporating Temperature and Superheat – Point 2.

Finally, Figure 5 shows the mass distribution in the evaporator for the Point 1. During all the simulation, the total mass is 120 grams. The initial vapor and liquid mass are 84 grams and 36 grams respectively. Therefore, in the steady state the vapor mass and the liquid mass are 68 grams and 53 grams respectively. For the Point 2 in the real transient the same values are found.

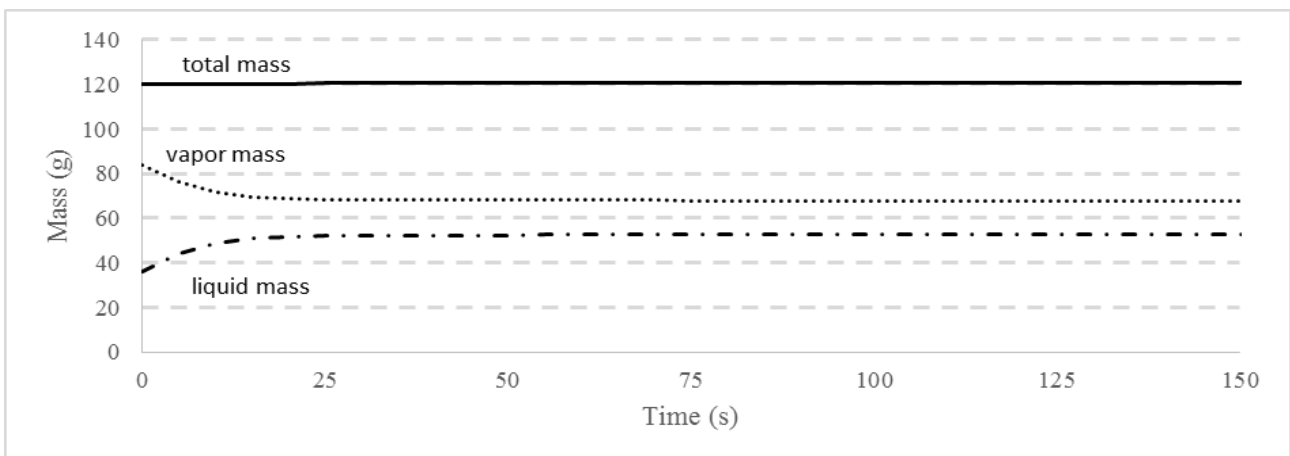


Figure 5. False Transient – Vapor mass, Liquid Mass and Total Mass in the Evaporator – Point 1.

The use of the false transient could be an interesting tool when the knowledge about the initial transient it is not important. For example, in a DX-SAHP if the objective is simulate the impact of the environment change, e.g. solar radiation, after the system operate in the steady state. In situations like that the use of the false transient could be minimize the simulation time. In addition, the problems of model convergences that occur frequently in the first instants of the real transient simulation are practically non-existent when the false transient simulation strategy is employed.

4. CONCLUSIONS

In this paper, the distributed model of a false transient achieves the steady state in a CO₂ DX-SAHP. It discussed if the system has the same environment conditions, the inlet and outlet evaporator mass flow rate is the same and the same mass is consider in the evaporator, a single steady state will be reached, regardless of the initial values chosen for the refrigerant temperature and liquid-vapor spatial distribution. The use of the false transient could be an interesting tool when the knowledge about the initial transient it is not important.

5. ACKNOWLEDGEMENTS

This work was supported by Fundação de Amparo à Pesquisa do Estado de Minas Gerais (FAPEMIG).

6. REFERENCES

- Cheng, L., Ribatski, G., Wojtan, L. and Thome, J.R., 2006. "New flow boiling heat transfer model and flow pattern map for carbon dioxide evaporating inside horizontal tubes". *International Journal of Heat and Mass Transfer*, Vol. 49, p. 4082–4094.
- Cheng, L., Ribatski, G., Quibe'n, J.M. and Thome, J.R., 2008. "New prediction methods for CO₂ evaporation inside tubes: Part I – A two-phase flow pattern map and flow pattern based phenomenological model for two-phase flow frictional pressure drops". *International Journal of Heat and Mass Transfer*, Vol. 51, p. 111–124.
- Duffie, J.A. and Beckman, W.A., 2006. *Solar Engineering of Thermal Processes*. Wiley, 3rd edition.
- Esbri, J.N., Milián, V., Mota-Babiloni, M., Molés, F. and Verdú, G., 2015. "Effect of mean void fraction correlations on a shell-and-tube evaporator dynamic model performance". *Science and Technology for the Built Environment*, Vol. 21, p. 1059–1072.
- Faria, R.N., Nunes, R.O., Koury, R.N.N. and Machado, L., 2016. "Dynamic modeling study for a solar evaporator with expansion valve assembly of a transcritical CO₂ heat pump". *International Journal of Refrigeration*, Vol. 64, p. 203–213.
- Huhtiniemi, I.K., Corradini, M. L., 1993. "Condensation in the presence of noncondensable gases". *Nuclear Engineering and Design*, Vol. 141, p. 429–446.
- Incropera, F.P. and DeWitt, D.P., 2002. *Fundamentals of Heat and Mass Transfer*. John Wiley & Sons, 5th edition.
- Kalogirou, S., 2009. *Solar Energy Engineering: Processes and Systems*. Elsevier, Burlington, 1st edition.
- Moreno-Rodríguez, A., González-Gil, A., Izquierdo, M. and Garcia-Hernando, N., 2012. "Theoretical model and experimental validation of a direct-expansion solar assisted heat pump for domestic hot water applications". *Energy*, Vol. 45, p. 704–715.
- Navarro-Esbri, J., Ginestar, D., Belman, J.M., Milián, V. and Verdú G., 2010. "Application of a lumped model for predicting energy performance of a variable-speed vapour compression system". *Applied Thermal Engineering*, Vol. 30, p. 286–294.
- Ozisik, M.N., 1985. *Heat Transfer, a Basic Approach*. McGraw-Hill, New York.
- Palyvos, J.A., 2008. "A survey of wind convection coefficient correlations for building envelope energy systems modeling". *Applied Thermal Engineering*, Vol. 28, p. 801–808.
- Rouhani, S.Z., Axelsson, E., 1970. "Calculation of void volume fraction in the subcooled and quality boiling regions". *International Journal of Heat and Mass Transfer*, Vol. 13, n.2, p. 383-393.
- Salazar, M. and Méndez, F., 2014. "PID control for a single-stage transcritical CO₂ refrigeration cycle". *Applied Thermal Engineering*, Vol. 67, p. 429-438.
- Span, R. and Wagner, W., 1996. "A new equation of regime for carbon dioxide covering the fluid region from the triple-point temperature to 1100 K at pressures up to 800 MPa". *Journal of Physical and Chemical Reference Data*, Vol. 25, p. 1509–1596.
- Zhou, G., Zhang, Y., Yang, Y. and Wang, X., 2010. "Numerical model for matching of coiled adiabatic capillary tubes in a split air conditioner using HCFC22 and HC290". *Applied Thermal Engineering*, Vol. 30, p. 1477-1487.

7. RESPONSIBILITY NOTICE

The authors are the only responsible for the printed material included in this paper.